ORIGINAL ARTICLE

Characterization of cardiac sarcoidosis in Iranian patients using cardiac magnetic resonance and positron emission tomography imaging techniques

Simin Almasi[1]*, Amir Azimi[2]*, Kiyan Heshmat-Ghahdarijani[2], Amir Ghaffari Jolfayi[2], Mahsa Ghorbani[2], Shahla Meshgi[2], Maedeh Dastmardi[3], Ghazaleh SalehAbadi[3], Ali Mohammadzadeh[2]

[1]Department of Rheumatology, Firoozgar Hospital, Iran University of Medical Sciences, Tehran, Iran, [2]Rajaie Cardiovascular, Medical and Research Center, Iran University of Medical Sciences, Tehran, Iran, [3]Department of Radiology, School of Medicine, Rajaei Cardiovascular, Medical and Research Center, Iran University of Medical Sciences, Tehran, Iran

*Both authors have contributed equally to this work and share first authorship

Background: Cardiac involvement in sarcoidosis is associated with high mortality but is often underrecognized due to diagnostic challenges. Advanced imaging modalities like Cardiac Magnetic Resonance (CMR) and Fluorodeoxyglucose Positron Emission Tomography (FDG-PET) are highly sensitive for detecting myocardial inflammation and scarring, aiding in the diagnosis and management of cardiac sarcoidosis. The objective of this study was to characterize the imaging features of cardiac sarcoidosis in Iranian patients using these advanced cardiac imaging modalities. **Materials and Methods:** This multicenter prospective study included 42 Iranian patients with biopsy-proven extracardiac sarcoidosis who met the Japanese Circulation Society criteria for cardiac involvement. All patients underwent CMR to evaluate myocardial function, edema, scarring, and strain. 28 patients also underwent FDG-PET/CT to assess active myocardial inflammation. **Results:** In our study of 42 cardiac sarcoidosis patients (50% male, mean age 47.14±14.33 years), CMR revealed reduced left ventricular ejection fraction (34.2±13.7%) in 83.3% of patients, with late gadolinium enhancement (LGE) present in 88.1%. LGE was most frequent in the basal anteroseptal and mid inferoseptal/anteroseptal segments, with midwall (35.5%) and subepicardial (23.7%) patterns predominating. Global strain analysis showed impaired values: longitudinal -10.08±4.14%, radial 15.38±8.55%, and circumferential -10.79±4.63%. Mean T1 and T2 values were 1054.60±50.98 ms and 52.59±4.53 ms, respectively. FDG-PET demonstrated active disease in 67.9% of cases, predominantly involving the apical septum, basal inferolateral, and mid inferolateral segments. The left anterior descending artery territory showed the highest involvement in both active inflammation (44.3% of affected segments) and scarring (39.2% of affected segments). **Conclusion:** CMR and FDG-PET provided comprehensive assessment of cardiac involvement in this Iranian cardiac sarcoidosis cohort, with predominant basal and lateral wall involvement. Regional differences highlight the importance of population-specific studies.

Key words: Cardiac magnetic resonance, cardiac sarcoidosis, imaging, Iranian, positron emission tomography

How to cite this article: Almasi S, Azimi A, Heshmat-Ghahdarijani K, Jolfayi AG, Ghorbani M, Meshgi S, *et al.* Characterization of cardiac sarcoidosis in Iranian patients using cardiac magnetic resonance and positron emission tomography imaging techniques. J Res Med Sci 2025;30:40.

INTRODUCTION

Sarcoidosis is a multisystem disorder with an unknown etiology characterized by the development of inflammatory noncaseating granulomas. The prevalence of sarcoidosis varies greatly between 50 and 160 per 100,000 population, depending on the region of the world. The clinical presentation is variable, and the diagnosis is usually based on a combination of clinical and radiological findings.[1-3]

Cardiac involvement in sarcoidosis, although often asymptomatic, is associated with high mortality rates. Autopsy studies suggest a 25% prevalence of cardiac involvement, but only 5%–10% of these cases

Access this article online

Quick Response Code:

Website: https://journals.lww.com/jrms

DOI: 10.4103/jrms.jrms_136_25

Address for correspondence: Prof. Ali Mohammadzadeh, Rajaei Cardiovascular, Medical and Research Center, Iran University of Medical Sciences, Tehran, Iran.
E-mail: mralimohammadzadeh@yahoo.com

Submitted: 22-Feb-2025; **Revised:** 06-May-2025; **Accepted:** 13-Jul-2025; **Published:** 24-Jul-2025

are symptomatic. Accurate diagnosis and determination of the extent of disease activity are essential to ensure timely treatment. Clinical presentations of cardiac sarcoidosis (CS) can range from incidental findings to heart failure, arrhythmias, and sudden death. CS is often under-recognized in clinical practice due to its diagnostic difficulty, which relies on integrating clinical, pathological, and advanced imaging data.[4-6]

While endomyocardial biopsy offers high specificity for diagnosing CS, its sensitivity is limited. Cardiac magnetic resonance (CMR) and fluorodeoxyglucose positron emission tomography (FDG-PET) are the most sensitive imaging modalities for detecting CS. Both FDG-PET and CMR can predict death and other major adverse cardiac events in CS.[7,8]

CMR imaging allows for the noninvasive diagnosis of subclinical or clinical CS and is the preferred method for evaluating suspected patients. Late gadolinium enhancement (LGE) is not specific for inflammation, but recent studies suggest that increased T2-weighted signals can detect myocardial edema, indicating inflammation in its early and potentially reversible stages. Myocardial strain imaging has also emerged as a useful tool for providing additional prognostic information beyond left ventricular ejection fraction (LVEF). Many patients with suspected CS benefit from the complementary information provided by CMR and PET. CMR provides information on scar presence and extent, whereas PET offers insights into myocardial inflammation's presence, extent, and severity.[9,10]

Recent literature has shown varying rates of CS progression across different countries. This variability highlights the need for region-specific studies to understand the disease better. Therefore, we aim to conduct a study for the first time that describes the imaging features of sarcoidosis patients specifically in the Iranian race using advanced cardiac imaging techniques.

METHODS

Study population

This study focused on patients with extracardiac biopsy-proven sarcoidosis who exhibited suspicion of cardiac involvement. Suspicion was based on the presence of cardiac symptoms such as dyspnea and palpitations or the emergence of new, unexplained atrioventricular block, atrial or ventricular arrhythmias, or left ventricular dysfunction. These clinical indicators necessitated further imaging to evaluate potential CS. These patients were referred from rheumatology centers to the two tertiary heart centers between 2021 and 2024. They underwent CMR and PET scans as part of the diagnostic process. The inclusion criteria were patients who met the diagnostic guidelines set forth by the Japanese Circulation Society (JCS) 2022 for CS.[11] The exclusion criteria included individuals with claustrophobia, renal impairment (defined as an estimated glomerular filtration rate <30 mL/min/1.73 m^2), coexisting cardiac conditions that might confound the sarcoidosis diagnosis, suboptimal imaging quality, and patients with a JCS score of 0 or 1, indicating no or low probability of CS. The study was conducted according to the principles of the Declaration of Helsinki and was approved by the local ethics committee of the participating center (Ethical code: IR.RHC.REC.1401.031).

Cardiac magnetic resonance image acquisition and analysis

CMR imaging was conducted using a 1.5 T Siemens Magnetom Aera machine (syngo MR XA20) from Siemens Medical Systems in Erlangen, Germany. A single operator (H. F., with over 10 years of experience in cardiac MR) performed all image acquisitions. The imaging protocol consisted of acquiring three long-axis views (four-, three-, and two-chamber) and a complete set of short-axis cine images using a steady-state free precession (SSFP) sequence. Subsequently, three short-axis sections (basal, mid, and apical) were imaged using a segmented inversion-recovery gradient-echo sequence, approximately 1–3 min after administering 0.1 mmoL/kg of intravenous gadolinium contrast (Gadoterate meglumine, marketed as Dotarem by Guerbet S. A., Paris, France) for early gadolinium enhancement. Finally, LGE images were obtained 15–20 min after contrast agent injection, covering three long-axis views and the full stack of short-axis views.

The modified look-locker inversion protocol with a 5 (3) 3 scheme was utilized for myocardial T1 mapping. The acquisition parameters included a pixel bandwidth of 977 Hz/pixel, an echo time of 1.12 ms, a flip angle of 35°, a matrix size of 256 × 144, and a slice thickness of 8 mm. For myocardial T2 mapping, three single-shot images were acquired at different preparation times (0, 24, and 55 ms). To account for motion, motion correction techniques were employed by estimating coefficients of the decay function used to estimate T2 times. The acquisition parameters consisted of an echo time of 1 ms, a repetition time of 2.4 ms, a flip angle of 70°, a matrix size of 160 × 105, and a slice thickness of 8 mm. To evaluate myocardial strain, a retrospective electrocardiogram (ECG)-gated cine SSFP sequence was employed with a breath-hold technique. The acquisition parameters involved an accumulation of repetition time of 40 ms, echo time of 1.3 ms, flip angle of 60°, section thickness of 6 mm, slice gap of 9 mm, field of view of 360 mm, and a matrix size of 256 × 208. LGE imaging was conducted using a breath-hold gradient-echo protocol with inversion recovery preparation. The acquisition

parameters included a repetition time of 700 ms, echo time of 4.33 ms, matrix size of 256 × 256, flip angle of 30°, slice thickness of 8 mm without any interslice gap, and a voxel size of 1.7 mm × 1.4 mm × 8 mm. Cine, strain, mappings, and LGE data were assessed using CVI42 software (Circle Cardiovascular Imaging, Calgary, Alberta, Canada) [Figure 1]. Two experienced observers, who were blinded to clinical outcomes, analyzed all CMR images. Patients exhibiting CMR abnormalities indicative of CS were categorized as CMR positive, whereas patients without any CMR abnormalities suggestive of CS were labeled as CMR negative.

Fluorodeoxyglucose-positron emission tomography/computed tomography image acquisition and analysis

The resting state 99 mTc sestamibi single-photon emission computed tomography myocardial perfusion imaging study was conducted using low-energy, high-resolution collimators. A noncircular, body-contouring 180° acquisition arc was employed, ranging from the right anterior oblique to the left posterior oblique. This was accompanied by a computed tomography (CT) acquisition with parameters of 16 effective milliampere-seconds (eff-mAs), 130 kilovolts (kV), and a matrix size of 512 × 512 for CT-based nonuniform attenuation correction. The imaging was performed using a dual-head gamma camera (Symbia T6, Siemens Healthcare). An FDG-PET study was conducted using the Siemens Biograph Horizon PET-CT system. Patients underwent fasting and appropriate dietary manipulation. Dedicated cardiac and whole-body PET-CT scans were obtained. Patients who displayed myocardial uptake on FDG-PET/CT were classified as PET positive [Figure 2].

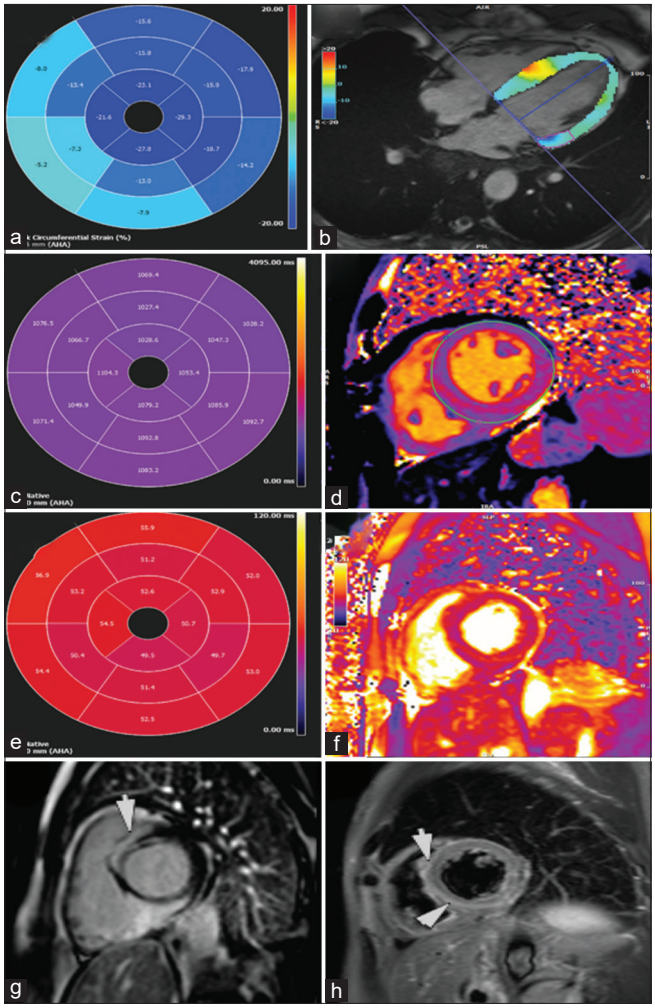

Figure 1: Cardiac magnetic resonance images a 58-year-old man suspected case of cardiac sarcoidosis (CS), (a and b) decrease in strain values in basal anteroseptal, inferoseptal and inferior regions, (c and d) demonstrate increase in T1 values in mentioned regions, (e and f) shows increase in T2 values in mentioned regions, (g) late gadolinium enhancement in basal anteroseptal region (white arrows), and (h) oedema in T2STIR in septal region

Data collection

The collection of patient data, including demographics, initial symptoms, and comorbidities such as hypertension, diabetes mellitus, and dyslipidemia, was systematically conducted utilizing a structured questionnaire. This questionnaire was administered to patients upon their arrival for imaging procedures. The evaluation of each patient's history of heart block was meticulously carried out by an experienced cardiovascular specialist. This process entailed a detailed review of the patient's previous medical records, which included the interpretation of historical ECGs and holter monitoring.

Statistical analysis

We employed SPSS (Version 26.0; IBM Corp., Chicago, IL, USA) for data summarization and statistical analysis. All categorical variables are presented as frequency (percentage), and summarized all continuous variables as mean ± standard deviation.

RESULTS

Patient selection

Our study was designed to prospectively identify and characterize patients with suspected cardiac involvement among those with biopsy-proven sarcoidosis. We recruited 68 individuals with confirmed sarcoidosis who were referred to the Shaheed Rajaie Cardiovascular, Medical and Research Center or Tehran Heart Center for further evaluation using advanced diagnostic imaging, including CMR and FDG-PET scans. Of these 68 patients, 7 did not meet the Japanese Ministry of Health and Welfare (JMHW) criteria for CS and were thus considered negative for cardiac involvement. An additional 17 patients displayed only one of the JCS criteria for CS. However, due to the incomplete fulfillment of all five necessary evaluations, their diagnoses could not be conclusively established as either meeting or not meeting the criteria. Therefore, the scope of our study was refined to focus on the 42 patients who clearly satisfied

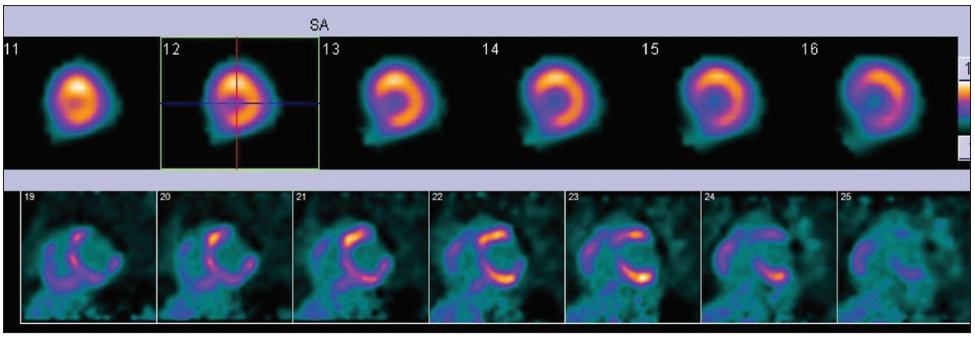

Figure 2: The Fluorodeoxyglucose (FDG)-positron emission tomography/computed tomography of the same patient, the rest 99m-Tc Sestamibi images show mild hypoperfusion of the septal, basal inferior, basal inferolateral segments. The FDG images show a mismatch with uptake inthe regions of hypoperfusion, as well as patchy uptake in the right ventricle

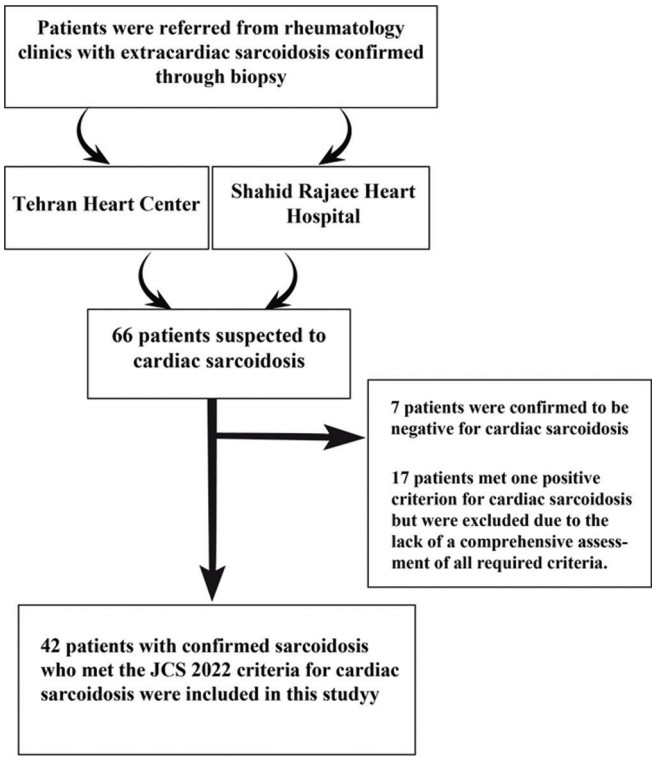

Figure 3: Flowchart of the patient selection process utilized in our study. JCS = Japanese Circulation Society

the JMHW criteria for CS. Figure 3 provides a detailed flowchart of the patient selection process utilized in our study.

Patient characteristics

In our multicenter descriptive study, data from 42 CS patients were analyzed, evenly distributed by gender with 21 males and 21 females, and an average age of 47.14 ± 14.33 years. Hypertension was present in nearly half the cohort, affecting 20 patients (47.6%), whereas diabetes mellitus and dyslipidemia were reported in 10 (23.8%) and 14 (33.3%) patients, respectively. Dyspnea was the primary symptom in 34 patients (80.9%), followed by palpitations in 14 cases (33.3%). Chest pain and syncope were relatively rare, each reported by two patients (4.6%). Conduction block was evident in the electrocardiographic history of 22 patients (52.4%).

Table 1 provides a comprehensive summary of the demographic and clinical and imaging characteristics of the patients included in the study.

Cardiac magnetic resonance imaging

CMR findings indicated a reduced LVEF in 35 patients (83.3%), with an average of 34.21% ± 13.71%. Average left ventricular end-diastolic and end-systolic volume indices were 95.57 ± 37.16 mL/m^2 and 66.80 ± 38.10 mL/m^2, respectively. The left and right atrial sizes averaged 21.61 ± 9.13 cm^2 and 16.87 ± 5.65 cm^2. Gadolinium enhancement, a marker of myocardial scarring, was observed in 37 patients (88.1%). Global longitudinal strain was −10.08% ± 4.14%, global radial strain 15.38% ± 8.55%, and global circumferential strain −10.79% ± 4.63%. Mean global T1 and T2 values were measured at 1054.60 ± 50.98 ms and 52.59 ± 4.53 ms.

In the segment-based analysis of 714 myocardial segments, scarring was identified in 186 segments (26.1%). The basal anteroseptal region (segment 2) showed the highest involvement with 29 affected segments, representing 15.6% of all scarred segments. This was followed by equal involvement of the midventricular inferoseptal (segment 9) and midanteroseptal (segment 8) regions, each with 20 affected segments (10.8%).

When analyzed by coronary territory distribution, the left anterior descending (LAD) artery territory showed the highest involvement with 73 segments (39.2% of affected segments), followed by the right coronary artery (RCA) territory with 66 segments (35.5%), and the left circumflex artery (LCX) territory with 47 segments (25.3%).

Table 1: Demographic, clinical, and imaging characteristics of the included patients

Demographics	Number of patients (%) or mean±SD
Sex (male)	21 (50)
Age	47.14±14.33
Primary symptom	
Dyspnea	34 (80.9)
Palpitations	14 (33.3)
Chest pain	2 (4.6)
Syncope	2 (4.6)
Comorbidity	
Hypertension	20 (47.6)
Diabetes mellitus	10 (23.8)
Dyslipidemia	14 (33.3)
Holter findings from history	
Heart block	22 (52.4)
CMR findings	
LVEF (%)	34.21±13.71
Reduced LVEF	35 (83.3)
Left ventricular end-diastolic volume index (mL/m^2)	95.57±37.16
Left ventricular end-systolic volume index (mL/m^2)	66.80±38.10
Left atrium diameter (mm)	21.61±9.13
Right atrium diameter (mm)	16.87±5.65
Global longitudinal strain (%)	−10.08±4.14
Global radial strain (%)	15.38±8.55
Global circumferential strain (%)	−10.79±4.63
Native T1 mapping value (ms)	1054.60±50.98
Native T2 mapping value (ms)	52.59±4.53
PET	
Positive tracer uptakes	19 (67.9)

CMR=Cardiac magnetic resonance; PET=Positron emission tomography; SD=Standard deviation; LVEF=Left ventricular ejection fraction

The midwall involvement of the myocardium was the most common scarring pattern in 66 segments (35.5% of all affected segments). Other patterns included subepicardial in 44 segments (23.7%), subendocardial in 24 segments (12.9%), and transmural in 23 segments (12.4%). Scarring extended from subepicardial to midwall in 18 segments (9.7%) and from subendocardial to midwall in 12 segments (6.5%). Figure 4a presents a summary of the CMR findings for the study's patient.

Positron emission tomography scans

PET imaging, performed in 28 patients, revealed active inflammatory disease in 19 cases (67.9%). Of the 476 myocardial segments analyzed, 97 (20.4%) showed positive FDG uptake. The distribution pattern showed predominant involvement of the apical septal region (segment 14) with 11 affected segments, followed by the basal inferolateral (segment 5) with 10 segments, and mid inferolateral (segment 11) with 9 segments.

The coronary territory analysis of active inflammation demonstrated predominant involvement of the LAD territory with 43 segments (44.3%), followed by the LCX territory with 31 segments (32.0%), and the RCA territory with 23 segments (23.7%). Figure 4b displays an overview of the PET scan results for the patients included in our study.

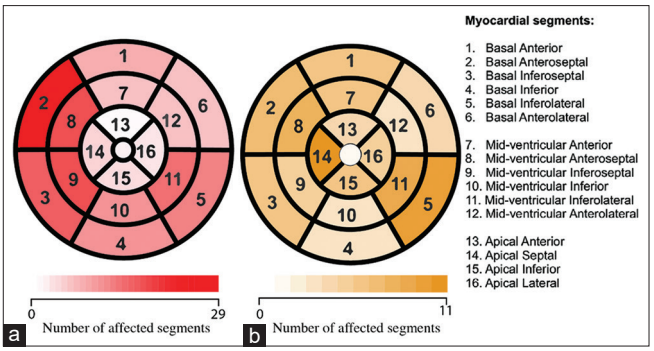

Figure 4: Distribution of cardiac involvement as detected by cardiac magnetic resonance imaging (a) and positron emission tomography scans (b). In both panels, darker shades correspond to areas of more frequent cardiac involvement

Concordance of late gadolinium enhancement and positron emission tomography findings

Among the 28 patients who underwent both imaging modalities, pattern matching analysis revealed concordant positive findings in 16 patients (57.1%). Seven patients (25.0%) showed positive LGE findings but negative PET results, whereas three patients (10.7%) demonstrated the opposite pattern. Concordant negative findings were observed in two patients (7.1%).

DISCUSSION

For the first time, this multicenter study aimed to characterize cardiac involvement in Iranian patients with biopsy-proven extracardiac sarcoidosis using advanced cardiac imaging with CMR and FDG-PET/CT. A total of 42 patients met the JCS criteria for CS and were included in the analysis. CMR revealed reduced LVEF (average 34.2%), LGE in 88.1% of patients, predominantly involving the basal anteroseptal and mid inferoseptal/anteroseptal segments, and abnormal global strains. FDG-PET/CT performed on 28 patients showed active CS in 67.9%, with the most frequently involved apical septum, basal inferolateral, and mid inferolateral segments. The LAD territory was the most affected by active inflammation on PET and scarring on CMR.

Our study utilized the 2022 guidelines from the JCS, for diagnosing and managing CS, incorporating the latest diagnostic technologies and an enhanced understanding of the disease's pathology. These updated guidelines emphasize the importance of advanced imaging techniques, such as FDG-PET and CMR. These methods provide superior diagnostic accuracy compared to traditional

Table 2: Detailed frequency of the different scarring patterns observed in cardiac magnetic resonance imaging conducted on patients with cardiac sarcoidosis

AHA 17-segment model	Midwall	Subepicardial	Subendocardial	Subepicardial to midwall	Subendocardial to midwall	Transmural
Basal anterior	2	2	2	3	0	0
Mid anterior	2	0	2	3	0	0
Apical anterior	0	0	1	0	0	0
Apex	0	0	1	0	0	0
Basal anteroseptal	18	6	2	3	0	0
Mid anteroseptal	12	4	2	1	1	0
Apical septal	3	1	1	0	0	0
Basal inferoseptal	9	4	2	1	1	1
Mid inferoseptal	9	4	2	1	2	2
Basal inferior	3	3	2	0	2	2
Mid inferior	3	5	1	0	0	3
Apical inferior	1	1	1	0	0	1
Basal inferolateral	0	4	2	2	1	5
Mid inferolateral	0	8	1	1	2	4
Apical lateral	0	0	0	0	1	2
Basal anterolateral	1	2	1	1	0	2
Mid anterolateral	1	0	1	2	2	1

AHA=American Heart Association

histological approaches, which are invasive and often limited by the disease's patchy nature. This advancement enables a more thorough assessment of myocardial inflammation and damage, thereby improving the management of CS.[11-14] The criteria are summarized in Table 2.

The pathophysiology of CS and its manifestations on imaging are closely linked to the disease's inflammatory and fibrotic processes. The chronic inflammation characteristic of the disease leads to myocardial scarring and fibrosis, where the fibrotic tissue replaces normal myocardial cells. CMR imaging is particularly valuable in detecting these changes through LGE techniques, which can identify areas of myocardial fibrosis or scarring. The granulomatous inflammation primarily affects the myocardium and can lead to localized inflammation. On PET scans, this inflammation is typically detected as increased uptake of FDG, indicating high glucose metabolism of inflammatory cells.[15]

The demographic characteristics of CS in this Iranian cohort revealed an equal gender distribution (50% male, 50% female), contrasting with international patterns where female predominance is typically observed in both the United States and Japanese populations.[16-18] While the mean age of 47.14 ± 14.33 years in this Iranian group broadly aligns with international data, it represents a somewhat younger demographic compared to Japanese registries, where peak diagnosis occurs between 60 and 64 years. Geographic and racial variations in CS have been well-documented, with US data showing higher prevalence among Black Americans, particularly in urban East Coast regions, whereas Japanese populations demonstrate remarkably high cardiac involvement rates of nearly 60% among sarcoidosis cases.[16-18]

LGE is the most distinctive CMR finding in CS. In the study by Coleman *et al*., the prevalence of LGE ranged from 13% to 89% across 10 individual studies included in their meta-analysis.[19] In our study, 37 (88.1%) patients had positive LGE, indicating regions of myocardial fibrosis or scarring due to granulomatous inflammation. This enhancement often appears patchy and is predominantly located in the mid-wall or subepicardial regions of the basal septum and lateral wall of the left ventricle.[20] Similarly, our findings showed the predominant LGE pattern was mid-wall and subepicardial in the basal anteroseptal and mid-inferoseptal regions.

CS may also present with increased signal intensity on T2-weighted images, reflecting myocardial edema and active inflammation.[21] Our study showed a slightly elevated T2 value of 52.59 ± 4.53 ms compared to the normal range in healthy individuals. Puntmann *et al*. also reported significantly increased T1 and T2 values in CS patients versus controls, although they did not provide the exact values.[22] Notably, Aquino *et al*. found that T2 > 49 ms was the most sensitive cutoff (92.9%) with a high negative predictive value (96.2%) for diagnosing CS.[23]

Studies have shown lower GLS and GCS rates in LGE-positive suspected CS patients due to myocardial fibrosis.[24,25] Our study, involving confirmed cases of CS,

demonstrated even lower mean GLS and GCS values, likely reflecting more advanced myocardial involvement and fibrosis in these patients with established cardiac sarcoid.

The meta-analysis found that 18F-FDG-PET/CT had a pooled sensitivity of 0.84% for detecting CS across 17 studies with 891 patients. In other words, the FDG-PET positive rate for CS was 84%.[26] In our study of 28 patients, 19 cases (67.9%) showed active disease on FDG-PET. FDG uptake in CS often involves the basal and lateral left ventricular walls, differentiating it from coronary artery disease, where uptake follows coronary territories. In our study, the apical septum was most frequently involved, followed by the basal inferolateral segments.

Limitation

Several limitations should be considered when interpreting our findings. First, not all patients underwent both CMR and PET imaging, with PET data available for only 28 out of 42 patients, potentially leading to an incomplete characterization of disease patterns in some cases. Second, the relatively small sample size of 42 patients, although representative of a tertiary referral center population, may limit the generalizability of our findings to the broader Iranian population with CS. Finally, selection bias may have been introduced as patients were recruited from tertiary cardiac centers, potentially overrepresenting more severe cases.

CONCLUSION

CMR and FDG-PET provided a comprehensive assessment of cardiac involvement in this Iranian CS cohort, with predominant basal and lateral wall involvement. Regional differences highlight the importance of population-specific studies.

Financial support and sponsorship

Nil.

Conflicts of interest

There are no conflicts of interest.

REFERENCES

1. Caforio AL, Pankuweit S, Arbustini E, Basso C, Gimeno-Blanes J, Felix SB, *et al*. Current state of knowledge on aetiology, diagnosis, management, and therapy of myocarditis: A position statement of the European Society of Cardiology Working Group on myocardial and pericardial diseases. Eur Heart J 2013;34:2636-48, 2648a-2648d.
2. Baughman RP, Field S, Costabel U, Crystal RG, Culver DA, Drent M, *et al*. Sarcoidosis in America. Analysis based on health care use. Ann Am Thorac Soc 2016;13:1244-52.
3. Jain R, Yadav D, Puranik N, Guleria R, Jin JO. Sarcoidosis: Causes, diagnosis, clinical features, and treatments. J Clin Med 2020;9:1081.
4. Nunes H, Freynet O, Naggara N, Soussan M, Weinman P, Diebold B, *et al*. Cardiac sarcoidosis. Seminars in respiratory and critical care medicine, 2010;31:428–41. [doi: 10.1055/s-0030-1262211].
5. Birnie D, Ha AC, Gula LJ, Chakrabarti S, Beanlands RS, Nery P. Cardiac sarcoidosis. Clin Chest Med 2015;36:657-68.
6. Matsui Y, Iwai K, Tachibana T, Fruie T, Shigematsu N, Izumi T, *et al*. Clinicopathological study of fatal myocardial sarcoidosis. Ann N Y Acad Sci 1976;278:455-69.
7. Roth D, Kadoglou N, Leeflang M, Spijker R, Herkner H, Trivella M. Diagnostic accuracy of cardiac MRI, FDG-PET, and myocardial biopsy for the diagnosis of cardiac sarcoidosis: A protocol for a systematic review and meta-analysis. Diagn Progn Res 2020;4:5.
8. Manabe O, Oyama-Manabe N, Aikawa T, Tsuneta S, Tamaki N. Advances in diagnostic imaging for cardiac sarcoidosis. J Clin Med 2021;10:5808.
9. Caobelli F, Cabrero JB, Galea N, Haaf P, Loewe C, Luetkens JA, *et al*. Cardiovascular magnetic resonance (CMR) and positron emission tomography (PET) imaging in the diagnosis and follow-up of patients with acute myocarditis and chronic inflammatory cardiomyopathy: A review paper with practical recommendations on behalf of the European Society of Cardiovascular Radiology (ESCR). Int J Cardiovasc Imaging 2023;39:2221-35.
10. Liang K, Nakou E, Del Buono MG, Montone RA, D'Amario D, Bucciarelli-Ducci C. The Role of cardiac magnetic resonance in myocardial infarction and non-obstructive coronary arteries. Front Cardiovasc Med 2021;8:821067.
11. Sato K, Kawamatsu N, Yamamoto M, Machino-Ohtsuka T, Ishizu T, Ieda M. Utility of updated Japanese circulation society guidelines to diagnose isolated cardiac sarcoidosis. J Am Heart Assoc 2022;11:e025565.
12. Kawai H, Sarai M, Kato Y, Naruse H, Watanabe A, Matsuyama T, *et al*. Diagnosis of isolated cardiac sarcoidosis based on new guidelines. ESC Heart Fail 2020;7:2662-71.
13. Terasaki F, Kusano K, Nakajima T, Yazaki Y, Morimoto SI, Culver DA, *et al*. The characteristics of Japanese guidelines on diagnosis and treatment of cardiac sarcoidosis compared with the previous guidelines. Sarcoidosis Vasc Diffuse Lung Dis 2022;39:e2022028.
14. Yoshinaga K, Miyagawa M, Kiso K, Ishida Y. Japanese guidelines for cardiac sarcoidosis. Ann Nucl Cardiol 2017;3:121-4.
15. Hulten E, Aslam S, Osborne M, Abbasi S, Bittencourt MS, Blankstein R. Cardiac sarcoidosis-state of the art review. Cardiovasc Diagn Ther 2016;6:50-63.
16. Cheng RK, Kittleson MM, Beavers CJ, Birnie DH, Blankstein R, Bravo PE, *et al*. Diagnosis and management of cardiac sarcoidosis: A scientific statement from the american heart association. Circulation 2024;149:e1197-216.
17. Iso T, Maeda D, Matsue Y, Dotare T, Sunayama T, Yoshioka K, *et al*. Sex differences in clinical characteristics and prognosis of patients with cardiac sarcoidosis. Heart 2023;109:1387-93.
18. Griffin JM. Sex differences in cardiac sarcoidosis. Heart 2023;109:1346-7.
19. Coleman GC, Shaw PW, Balfour PC Jr., Gonzalez JA, Kramer CM, Patel AR, *et al*. Prognostic value of myocardial scarring on CMR in patients with cardiac sarcoidosis. JACC Cardiovasc Imaging 2017;10:411-20.
20. Komada T, Suzuki K, Ishiguchi H, Kawai H, Okumura T, Hirashiki A, *et al*. Magnetic resonance imaging of cardiac sarcoidosis: An evaluation of the cardiac segments and layers that exhibit late gadolinium enhancement. Nagoya J Med Sci 2016;78:437-46.
21. Vignaux O, Dhote R, Duboc D, Blanche P, Devaux JY, Weber S, *et al*. Detection of myocardial involvement in patients with sarcoidosis applying T2-weighted, contrast-enhanced, and cine magnetic

resonance imaging: Initial results of a prospective study. J Comput Assist Tomogr 2002;26:762-7.
22. Puntmann VO, Isted A, Hinojar R, Foote L, Carr-White G, Nagel E. T1 and T2 mapping in recognition of early cardiac involvement in systemic sarcoidosis. Radiology 2017;285:63-72.
23. Aquino G, Chamberlin J, Wortham A, Rieter W, James E, Houston BA, *et al*. Quantitative T2 mapping to diagnose cardiac sarcoidosis and predict incident heart failure. Circulation 2021;144 Suppl_1:A10664.
24. Dabir D, Meyer D, Kuetting D, Luetkens J, Homsi R, Pizarro C, *et al*. Diagnostic value of cardiac magnetic resonance strain analysis for detection of cardiac sarcoidosis. Rofo 2018;190:712-21.
25. Watanabe Y, Nishii T, Shimoyama S, Ito T, Mori S, Kono AK, *et al*. Focal myocardial damage in cardiac sarcoidosis characterized by strain analysis on magnetic resonance tagged imaging in comparison with fluorodeoxyglucose positron emission tomography accumulation and magnetic resonance late gadolinium enhancement. J Comput Assist Tomogr 2018;42:607-13.
26. Kim SJ, Pak K, Kim K. Diagnostic performance of F-18 FDG PET for detection of cardiac sarcoidosis; A systematic review and meta-analysis. J Nucl Cardiol 2020;27:2103-15.